

RNA-Binding to Archaeal RNA Polymerase Subunits F/E: A DEER and FRET Study

Dina Grohmann,[†] Daniel Klose,[‡] Johann P. Klare,[‡] Christopher W. M. Kay,[†] Heinz-Jürgen Steinhoff,[‡] and Finn Werner^{*†}

Institute of Structural and Molecular Biology, University College London, Darwin Building, Gower Street, London WC1E 6BT, United Kingdom, and Department of Physics, University of Osnabrück, Barbarastrasse 7, 49076 Osnabrück, Germany

Received February 26, 2010; E-mail: werner@biochem.ucl.ac.uk

DNA-dependent RNA polymerases (RNAPs) are complex multisubunit enzymes that facilitate transcription of all cellular genomes. The archaeal RNAP and eukaryotic RNAP are closely related in terms of subunit composition, ternary architecture, and requirements for basal transcription factors. Recently hyperthermophilic archaeal RNAPs have emerged as versatile model systems for the less tractable mesophilic eukaryotic RNAPII.^{1,2} During transcription RNAP interacts with double-stranded DNA, a 9 base pair DNA/RNA hybrid, and the nascent RNA chain. Biochemical studies have shown that the eukaryotic RNAPII subunits RPB4/7 and their archaeal homologues F/E bind the emerging RNA transcript in a nonsequence-specific manner over a range of approximately 20 nucleotides.^{3,4} This interaction stimulates the processivity of the archaeal RNAP.⁵ During transcription initiation, prior to RNA synthesis, F/E facilitates interaction with the basal transcription factor TFE and stimulates DNA-strand separation.^{6,7} The molecular mechanisms that underlie the interplay between TFE, F/E and RNA during transcription are poorly understood but are likely to involve dynamic conformational changes of the RNAP–nucleic acid complex.⁸ Subunits F/E form a stable heterodimer⁹ that associates stably with the RNAP core¹⁰ (Figure 1a). Structural and biophysical studies have provided insights into the topology of downstream and upstream DNA and the DNA/RNA hybrid in the context of the elongating RNAP.^{11,12} However, the nascent transcript and its interaction with F/E-like subunits have not yet been captured.

To characterize the interaction between subunits F/E and RNA in greater detail, we carried out an equilibrium fluorescence titration monitoring the fluorescence signal of a Cy3-labeled 27nt RNA upon addition of increasing amounts of subunits F/E (Figure 1b). The addition of F/E led to an increase of fluorescence, and fitting of the data yielded a dissociation constant of 0.34 (± 0.06) μM , which is in good agreement with semiquantitative studies using electrophoretic mobility shift assays (0.54 μM).³ The accurate determination of the affinity between RNA and F/E was essential to choose the appropriate conditions for the subsequent distance measurements in the presence and absence of RNA.

In this study we have employed pulsed double electron–electron resonance (DEER)¹³ and fluorescence resonance energy transfer (FRET) to probe for subtle alterations in the F/E structure upon binding of RNA. Both techniques report reliably on distances and changes thereof.^{13–15} We introduced single cysteine residues at positions 36 or 63 in subunit F and 49, 65, or 123 in subunit E, taking advantage of the fact that F and E can be expressed in a recombinant form, purified, and labeled individually prior to heterodimerization. These labeling positions were chosen because (i) they provide a good spatial

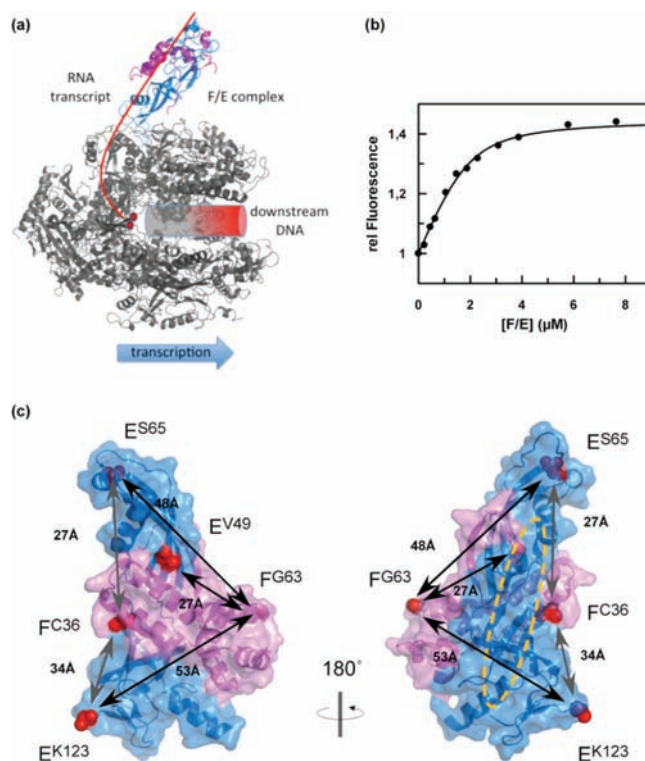


Figure 1. (a) Sketch of the transcription elongation complex. The archaeal RNAP is represented by the *S. shibatae* X-ray structure (PDB: 2WAQ,⁸ gray). RNAP subunits F and E are highlighted in magenta and blue. The path of the RNA transcript is indicated with a red dotted line, and the downstream duplex DNA binding channel is depicted as a cylinder. (b) Equilibrium titration of Cy3-labeled RNA (50 nM) with subunits F/E at 65 °C. Analysis of the data using a single-site binding model yielded a K_d of 0.34 (± 0.06) μM . (c) The probe derivatization sites are highlighted as red spheres in the crystal structure of the F/E complex⁹ (PDB: 1G03). The probe interactions are indicated with double headed arrows ($C\beta$ – $C\beta$ distances in angstrom). The location of the RNA binding interface is indicated with a yellow dashed circle.

coverage along both vertical and horizontal axes of the F/E complex (see Figure 1c) so that possible conformational changes in either direction could be monitored and (ii) they do not obstruct RNA binding (Figure 1c).^{3,5}

This approach allowed labeling with either nitroxide spin-label (MTSSL, the resulting spin label side chain is denoted R1) or the desired donor–acceptor fluorophor combination suitable for FRET at chosen sites in F or E. The structural and functional integrity of the labeled F/E complexes was ascertained in transcription elongation assays.⁵

Figure 2 illustrates the resulting DEER data for two double spin labeled F/E variants in the presence and absence of RNA. The chosen protein and RNA concentration ensured complete saturation

[†] University College London.

[‡] University of Osnabrück.

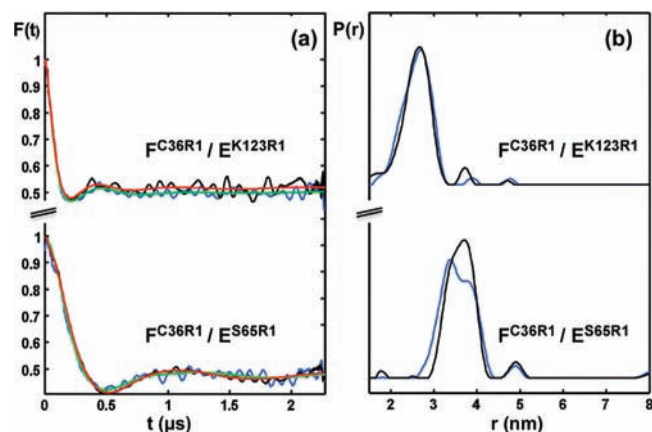


Figure 2. (a) Four-pulse DEER (16, 32 ns for $\pi/2$, π pulses and a frequency offset of 65 MHz pumping on the center of the nitroxide spectrum) form factors $F/E \pm$ RNA (blue and black, with the respective fits in green and red) after correction with a homogeneous 3D background, temperature $T = 50$ K. (b) DEER interspin distance distributions obtained by Tikhonov Regularization of the traces in (a) for $F/E \pm$ RNA (blue and black, respectively).

of F/E with RNA according to the affinity data derived from the equilibrium binding studies. The DEER distance distributions obtained by Tikhonov Regularization¹³ result in a single interspin distance of 27 ± 3 Å for F^{C36R1}/E^{C123R1} and 36 ± 4 Å for F^{C36R1}/E^{C65R1} . These distances correspond well to the $C\beta-C\beta$ distances in the F/E structure⁹ [PDB: 1GO3] (27 Å for F^{C36}/E^{K123C} and 34 Å for F^{C36}/E^{S65C}). The presence of RNA did not alter the interspin distance distributions significantly as judged by the form factors (Figure 2b). The result indicates that no gross structural rearrangement of F/E occurs upon RNA binding.

Our model organism *M. jannaschii* is viable between 48 and 94 °C. Therefore, we also performed FRET measurements of fluorescently labeled F/E complexes at the biologically relevant elevated temperature of 65 °C. F/E complexes F^{C63}/E^{C49} , F^{C63}/E^{C65} , and F^{C63}/E^{C123} were labeled with the donor fluorophor Alexa350 in subunit F at position 63 and with the acceptor fluorophor Alexa488 in subunit E at three different positions (49, 65, and 123). The emission spectra of all single and double labeled F/E complexes are shown in Figure 3. In the presence of the acceptor the donor fluorescence decreased and the acceptor emission increased accordingly indicating a high FRET efficiency. A distinct FRET signal is a prerequisite to monitor subtle changes in FRET efficiencies and thereby the distances between two probes. We calculated the interprobe distances from the decrease in donor emission using the Förster equation ($F^{G63C}-E^{V65C}$, $-E^{K123}$, $-E^{V49C}$ are 52 ± 2 , 53 ± 5 , and 46 ± 1 Å, respectively; X-ray [pdb 1GO3]: 48.2, 52.8, and 27.4 Å). The discrepancy between the measured $F^{G63C}-E^{V49C}$ distance and the X-ray structure is likely to be due to the relatively long Förster radius of the Alexa 350–488 pair ($R_0 = 50$ Å) compared to the distance between the probes (27.4 Å). The addition of RNA at saturating concentrations (20 μ M) to the donor–acceptor labeled F/E complexes had no influence on the relative donor and acceptor fluorescence intensities. Both FRET and DEER data are in good agreement and support the hypothesis that RNA binding has no influence on the overall structure of F/E.

In summary, we have shown that interspin distance distributions within the archaeal F/E complex can be accurately determined by DEER. Likewise, FRET can provide information about the structural flexibility of a subcomplex of the RNAP machinery, or the lack of flexibility. Our results demonstrate that RNAP subunits F/E are conformationally stable upon RNA binding, which suggests that the F/E complex acts as a *rigid* guiding rail that directs the emerging RNA

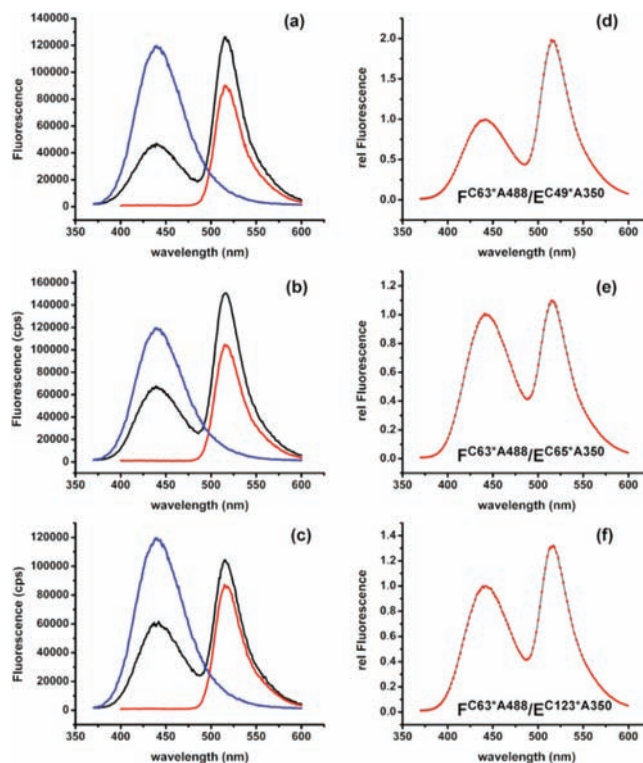


Figure 3. FRET within the F/E complex. (a–c) The fluorescence emission spectra are shown for donor only ($F^{C63}/E^{C49/A350}$, blue line), acceptor only ($F^{C63/A488}/E^{C49}$, red line), and donor–acceptor (DA) labeled F/E (black line) varying the position of the donor located in E (a: C49, b: C65, c: C123). (d–f) Fluorescence emission spectra of DA labeled F/E in the presence (red dashed line) or absence (gray line) of a 27nt RNA (20 μ M). The protein concentration was 50 nM, and the excitation was carried out at 320 nm.

away from the RNAP. This could possibly prevent the entanglement of the transcript with the DNA template during transcription. However, the results presented here do not rule out a movement of F/E as a rigid body relative to the RNAP core (Figure 1), which in turn could trigger a conformational change within the RNAP.

Acknowledgment. Research at the ISMB was funded by project grants from the Wellcome Trust (079351/Z/06/Z) and BBSRC (BB/E008232/1) to Finn Werner. Work at the University of Osnabrück was funded by DFG SFB 431 P18.

References

- Werner, F. *Mol. Microbiol.* **2007**, *65*, 1395–404.
- Werner, F.; Weinzierl, R. O. *Mol. Cell* **2002**, *10*, 635–46.
- Meka, H.; Werner, F.; Cordell, S. C.; Onesti, S.; Brick, P. *Nucleic Acids Res.* **2005**, *33*, 6435–44.
- Ujvari, A.; Luse, D. S. *Nat. Struct. Mol. Biol.* **2006**, *13*, 49–54.
- Hirtreiter, A.; Grohmann, D.; Werner, F. *Nucleic Acids Res.* **2010**, *38*, 585–96.
- Andrecka, J.; Lewis, R.; Bruckner, F.; Lehmann, E.; Cramer, P.; Michaelis, J. *Proc. Natl. Acad. Sci. U.S.A.* **2008**, *105*, 135–40.
- Werner, F.; Weinzierl, R. O. *Mol. Cell Biol.* **2005**, *25*, 8344–55.
- Korkhin, Y.; Unligil, U. M.; Littlefield, O.; Nelson, P. J.; Stuart, D. I.; Sigler, P. B.; Bell, S. D.; Abrescia, N. G. *PLoS Biol.* **2009**, *7*, e102.
- Todone, F.; Brick, P.; Werner, F.; Weinzierl, R. O.; Onesti, S. *Mol. Cell* **2001**, *8*, 1137–43.
- Grohmann, D.; Hirtreiter, A.; Werner, F. *Biochem. J.* **2009**, *421*, 339–43.
- Kettenberger, H.; Armache, K. J.; Cramer, P. *Mol. Cell* **2004**, *16*, 955–65.
- Andrecka, J.; Treutlein, B.; Arcusa, M. A.; Muschiello, A.; Lewis, R.; Cheung, A. C.; Cramer, P.; Michaelis, J. *Nucleic Acids Res.* **2009**, *37*, 5803–9.
- Pannier, M.; Veit, S.; Godt, A.; Jeschke, G.; Spiess, H. W. *J. Magn. Reson.* **2000**, *142*, 331–340.
- Jeschke, G.; Chechik, V.; Ionita, P.; Godt, A.; Zimmermann, H.; Banham, J.; Timmel, C. R.; Hilger, D.; Jung, H. *Appl. Magn. Reson.* **2006**, *30*.
- Heyduk, T. *Curr. Opin. Biotechnol.* **2002**, *13*, 292–6.

JA101663D